A feedforward deflection compensation scheme coupled with an offline path planning for robotic friction stir welding

Komlan Kolegain, Jean-François Léonard, Sandra Zimmer-Chevret, Amarilys Ben Attar, Gabriel Abba

A feedforward deflection compensation scheme coupled with an offline path planning for robotic friction stir welding ⋆

K. Kolegain * **F. Leonard** ** **S. Zimmer-Chevret** **
A. Ben Attar * **G. Abba** **

* *Institut de Soudure, 57420 Goin, France, (e-mail: k.kolegain@isgroupe.com, a.benattar@isgroupe.com)*
** *Arts et Métiers ParisTech, Université de Lorraine, Design, Manufacturing and Control Laboratory (LCFC), 57078 Metz Cedex 3, France, (e-mail: francois.leonard@univ-lorraine.fr, sandra.chevret@ensam.eu, gabriel.abba@univ-lorraine.fr)*

Abstract: Robotic friction stir welding is an innovative process which allows the welding of aluminum workpieces with robots. With their six-axis, serial industrial robots allow the welding of three-dimensional complex geometries but, under high load induced by the process, they undergo deflection due to their limited stiffness. Position and orientation deviations of the end effector are observed during welding experiments leading to weld defects. In this paper, a feedforward compensation technique based on a deflection model is implemented to compensate the deviations. This technique is coupled with an offline path planning methodology based on Bézier curves. The methodology is validated by performing an arc of circular helix welding path. High position and orientation accuracy are achieved and defect-free weld is performed.

Keywords: Robotic friction stir welding, feedforward technique, robot deflection, welding path compensation, Bézier curves.

1. INTRODUCTION

Friction Stir Welding (FSW) process consists of a tool composed of a pin and a shoulder put in rotation and plunged between two clamped parts. Then, the tool is moving along the joint line with the shoulder in contact with the parts surface inducing high forces and frictional heat during the process. A general description of the FSW process can be found in (Besharati-Givi and Asadi (2014)). It is a solid state welding process which allows the welding of aluminum materials and dissimilar materials. Aerospace and automotive industries are interested in this welding technology (Lyles et al. (2016), Kusuda (2013)). Dedicated machines are commonly used as FSW machines but they require high investment costs. To reduce the investments costs, robots can be used as FSW machines. Cook et al. (2004), Soron and Kalaykov (2006), Zaeh and Voellner (2010) used serial manipulator robot with a force feedback control to perform 2D and 3D welding paths. A review of machines and control system for FSW can be found in Mendes et al. (2016). Six-axis serial industrial robots allow the welding of complex geometries but they undergo deflection under the high process forces applied during the welding. This leads the welding tool to deviate in the lateral direction to the welding direction (Voellner et al. (2007), De Backer et al. (2010)). To perform FSW, the tool is oriented according to the process specifications. At each point of the seam, the tool has to be inclined in the opposite welding direction with an angle between the tool center line and the normal vector to the surface called tilt angle (Fig.1). The tool can be also inclined with an angle in the perpendicular plane to the welding direction called side tilt angle. Under high process forces, the welding tool orientation can be wrong. Thus, the tilt and the side-tilt angles must be correctly maintained during the welding. Otherwise, defects can be observed in the weld seam as described by Shultz et al. (2010) and Zimmer-Chevret et al. (2014). Many research works found in the literature propose compensation techniques to correct the tool lateral deviation, but not the tool wrong orientation. Two categories of techniques have been found: the online technique and the offline technique. The online compensation technique is based on a feedback control and the

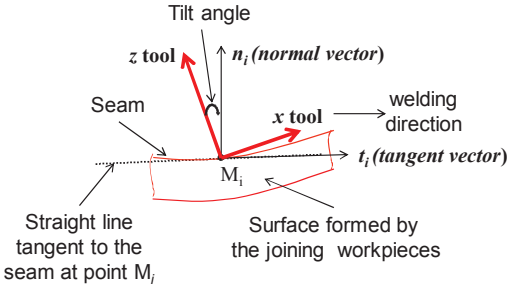

Fig. 1. FSW tool frame orientation illustration

⋆ The publication is funded by the "Office National d'Etudes et de Recherches Aérospatiales (O.N.E.R.A.)" via the project "NOUvelle Génération d'Assemblage aéronauTique (NOUGAT)".

compensation is done in real time using sensors (De Backer et al. (2012)) or nonlinear discrete observer (Qin et al. (2014), Qin et al. (2016)). These methods gave good results in 2D welding but have not validated in the welding of 3D complex paths. The offline compensation technique is based on the knowledge of the tool deviation before performing the welding. The classical trial/error method is often used. It consists of performing a first experiment, measuring the deviation and integrating the measured deviation during the next experiment. This method is not robust and can not be used in an industrial environment. Another offline technique is based on a feedforward control technique. The tool deviations are estimated with a stiffness model. This technique was used by Belchior et al. (2013) for robotic sheet forming and Tyapin et al. (2015), Cortsen and Petersen (2012) for robotic milling. Similar to these works, we propose to use the feedforward control technique to compensate simultaneously the tool lateral deviation and the wrong orientation of the tool of three-dimensional welding paths. By knowing the deflections before performing welding, these deflections can be integrated in the robot program. Thus, a modified or suitable path composed of the desired path and the deflections is programmed instead of programming only the desired welding path.

The modified path can be generated by mirroring the points contained in the robot program generated by an offline programming software (Klimchik et al. (2012), Bauer et al. (2013)). In this work, we propose to generate the robot program by approximating the modified path with parametric curves such as Bézier curves, B-splines or Non-Uniform Rational Basis Spline (NURBS). Parametric curves were used to plan paths for different applications. Giberti et al. (2017) used Bézier curves to plan a path for robotic additive manufacturing, Neubauer and Müller (2015) used B-splines for a polishing application, Jahanpour et al. (2016) used NURBS for a machining application.

In this paper, Bézier curve is used to generate the modified tool path for an arc of circular helix welding path. Being infinitely derivable, Bézier curves allow the planning of a smooth path. The low order obtained for the approximation of the arc of circular helix path allows us to use Bézier curves rather than using B-splines or NURBS. For other complex paths which need high order Bézier curves, B-splines or NURBS can be investigated.

The validation of the proposed methodology on the arc of circular helix welding path shows the effectiveness of the methodology. High position and orientation accuracy were achieved and defect-free weld was performed. The deflection model used for the feedforward compensation is described in Section 2. In Section 3, the proposed methodology to plan an RFSW path using Bézier curves is detailed. In Section 4, the welding experiments are presented and the results are discussed. Conclusions and future work are presented in Section 5.

2. ROBOT MODELING

The robot used in this work is a KUKA KR 500-2MT industrial robot. The models needed for this work are kinematic models and a deflection model. All numerical values of models parameters used in this paper can be found in Qin et al. (2016).

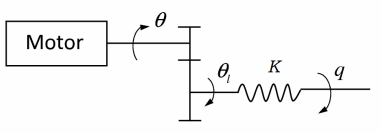

Fig. 2. One-dimensional torsional deformation model of a gearbox

2.1 Kinematic models

Forward and inverse kinematic models define the relationship between the joints angles and the pose (position and orientation) of the tool and vice versa. The detailed expressions of the kinematics models of the robot Kuka KR 500-2 MT are given by Qin (2013).

2.2 Cartesian deflection model

The cartesian deflection model define the relationship between the FSW load and the corresponding tool deviation in the operational space. Under FSW load, the robot applies a wrench W of forces and torques on the external environment. This wrench is expressed as:

$$\mathbf{W} = [F_x\, F_y\, F_z\, T_x\, T_y\, T_z]^\top \tag{1}$$

where F_x, F_y and F_z are the forces acting by the FSW tool on the workpiece; the torques T_x and T_y are negligible and the torque T_z is due to the rotation of the spindle.

Under the assertion that the deformation of the robot is mainly located on the joint axes Dumas et al. (2011), we define the model of torsional deformation given in Fig. 2. This model supposes that all deformations can be located on the output of the gearboxes. The identification method of Jubien et al. (2014) is used to determine the numerical values of the joint stiffness matrix $\boldsymbol{K}$ of the Kuka KR500-2MT robot (Table 1). The relation between the gearbox output torque vector Γ and the joint angular deflection is given by:

$$\boldsymbol{\Gamma} = \boldsymbol{K}(\boldsymbol{N}^{-1}\boldsymbol{\theta} - \boldsymbol{q}) = \boldsymbol{K}\Delta\boldsymbol{q} \tag{2}$$

where $\mathbf{q} = [q_1\, q_2\, q_3\, q_4\, q_5\, q_6]^\top$ is vector of angular positions of the joint, $\boldsymbol{\theta}_l = \boldsymbol{N}^{-1}\boldsymbol{\theta}$ is the angular position after gear reduction and $\Delta\boldsymbol{q}$ is the joint deflection of the gearbox output.

A general form of the robot's dynamic model (Khalil and Dombre (2004)) can be expressed as:

$$\boldsymbol{\Gamma} = \boldsymbol{D}(\boldsymbol{q})\ddot{\boldsymbol{q}} + \boldsymbol{H}(\boldsymbol{q}, \dot{\boldsymbol{q}}) + \boldsymbol{F}_f(\dot{\boldsymbol{q}}) + \boldsymbol{J}^\top(\boldsymbol{q})\boldsymbol{W} \tag{3}$$

where $\boldsymbol{D}(\boldsymbol{q})$ is the symmetric, uniformly positive defined and bounded inertia matrix of the robot and $\boldsymbol{H}(\boldsymbol{q}, \dot{\boldsymbol{q}})$ represents the contribution due to centrifugal, Coriolis and gravitational forces, $\boldsymbol{F}_f(\dot{\boldsymbol{q}})$ is the vector of friction torque

Table 1. Joint stiffness parameters of Kuka robot KR500-2MT (Qin et al. (2016))

Parameters	Value(Nm/rad)	Parameters	Value(Nm/rad)
K_1	3.8×10^6	K_4	5.6×10^5
K_2	6.6×10^6	K_5	6.6×10^5
K_3	3.9×10^6	K_6	4.7×10^5

applied on the joints, $\boldsymbol{J}^\top(\boldsymbol{q})$ is the Jacobian matrix and vectors $\dot{\boldsymbol{q}}$ and $\ddot{\boldsymbol{q}}$ represent joint velocities and accelerations.

Under low advance speed FSW experiments, the joints velocities and acceleration are relatively low. Thus, the inertia, centrifugal, Coriolis and friction terms can be neglected and (3) is reduced to:

$$\boldsymbol{\Gamma} = \boldsymbol{J}^\top(\boldsymbol{q})\boldsymbol{W} + \boldsymbol{H}(\boldsymbol{q}, \boldsymbol{0}) \tag{4}$$

where $\boldsymbol{H}(\boldsymbol{q}, \boldsymbol{0})$ represents the gravitational forces vector. The deflections in the operational space are obtained by:

$$\begin{bmatrix} \Delta \boldsymbol{P} \\ \Delta \boldsymbol{\Theta} \end{bmatrix} = \boldsymbol{L}_a \, \boldsymbol{J}(\boldsymbol{q}) \, \Delta \boldsymbol{q} \tag{5}$$

where $\Delta \boldsymbol{P} = [\Delta x \; \Delta y \; \Delta z]^\top$ is the deflection of the tool position, $\Delta \boldsymbol{\Theta} = [\Delta A \; \Delta B \; \Delta C]^\top$ is the deflection of the tool orientation and $\boldsymbol{L}_a$ is a matrix which defines the relation between the angular variation around the robot base frame and yaw, pitch and roll angles variation denoted A, B, C for the Kuka robot (Khalil and Dombre (2004)). We suppose here that the wrench W is known. The deflections along a welding path can be calculated using (6). These deflections represent the feedforward command vector.

$$\begin{bmatrix} \Delta \boldsymbol{P} \\ \Delta \boldsymbol{\Theta} \end{bmatrix} = \boldsymbol{L}_a \, \boldsymbol{J}(\boldsymbol{q}) \, \boldsymbol{K}^{-1} \left(\boldsymbol{J}^\top(\boldsymbol{q}) \, \boldsymbol{W} + \boldsymbol{H}(\boldsymbol{q}, \boldsymbol{0}) \right) \tag{6}$$

3. PATH PLANNING METHODOLOGY

The proposed offline methodology consists on generating a modified tool positions and orientation angles from CAD models. It starts with the extraction of geometrical information from the welding path defined in the CAD model of workpieces. An explicit equation of the path can be obtained. In the most of cases, the whole welding path can not be modeled by an explicit equation. In a CAD software, $m+1$ positions coordinates (x, y, z) of the welding path can be obtained by discretizing the path. Therefore, we propose to get the whole path equation by approximating the positions coordinates using Bézier curves.

Bézier curves are polynomial parametric curves which can be used to model complex paths. An n^{th}-order Bézier curve $P(u)$ is defined by:

$$P(u) = \sum_{i=0}^{n} P_i \frac{n!}{i!(n-i)!} u^i (1-u)^{n-i} \tag{7}$$

where u is a normalized parameter and $P_i \in \mathbb{R}^n$ are the control points.

Consider $X = [x_0 \cdots x_m]^\top$, $Y = [y_0 \cdots y_m]^\top$ and $Z = [z_0 \cdots z_m]^\top$, three vectors obtained from x, y and z coordinates of $m+1$ given points. The parameter u must be contained in $[0, 1]$. Either the uniform parametrization method or the chord length parametrization method can be used to get the parameter u.

Defined for all $i \in [0 \cdots m]$ and, for example, consider Z_b, the Bézier approximation of the z coordinates:

$$Z_b(u_i) = \sum_{i=0}^{n} P_{iz} B_i^n(u_i) \tag{8}$$

where $B_i^n(u) = \frac{n!}{i!(n-i)!} u^i (1-u)^{n-i}$. Then, the control points P_{iz} are obtained by solving a minimization problem

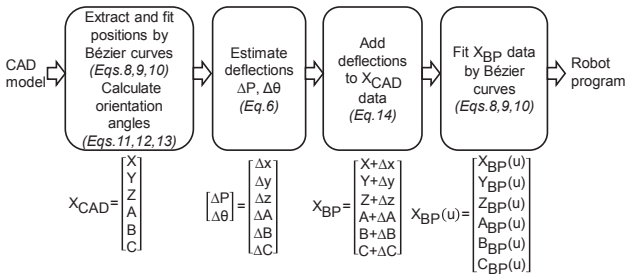

Fig. 3. Path planning methodology

defined by $\min \parallel Z - Z_b \parallel$. For $m \gg n$, the least squares method can be used to obtain:

$$P_z = [P_{0z} \cdots P_{nz}]^\top = \left(M^\top M\right)^{-1} M^\top Z \tag{9}$$

where $M = \begin{bmatrix} B_0^n(u_0) & \cdots & B_n^n(u_0) \\ \vdots & \ddots & \vdots \\ B_0^n(u_m) & \cdots & B_n^n(u_m) \end{bmatrix}$

Once the coefficients P_z are determined, the Bézier function Z_b which approximate the z coordinate can be computed. Afterwards, the maximum error due to the approximation can be calculated by the relation.

$$e_z = \max_{i \in [0,m]} \left(Z_b(u_i) - Z(u_i) \right) \tag{10}$$

If the maximum error is too high for an n^{th} order Bézier function, one can increase the order to $n+1$ until the error is lower than a defined constant ξ. This method of fitting z coordinate by Bézier curve can also be used to fit x and y positions and can be extended to orientation angles.

After the approximation of the position coordinates by Bézier curves, the orientation angles of the welding tool are calculated by defining a Darboux mobile frame using (11), (12) and (13). Suppose that $C(u) = (x(u), y(u), z(u))$ represents the Bézier functions of a welding path position coordinates where u is a normalized parameter. The Darboux mobile frame is defined at each point of the path by $F = (C(u), t, b, n)$ where t is the tangent vector, n the normal vector to the surface and b the binormal vector. The tangent vector t is calculated as:

$$t = \frac{\frac{dC(u)}{du}}{\parallel \frac{dC(u)}{du} \parallel} \tag{11}$$

where $\parallel \cdot \parallel$ represent the 2-norm. Consider $S(u, v) = (x(u, v), y(u, v), z(u, v))$ a parametrized surface in which the welding path is defined. The normal vector n is calculated as:

$$n = \frac{\frac{\partial S}{\partial u} \wedge \frac{\partial S}{\partial v}}{\parallel \frac{\partial S}{\partial u} \wedge \frac{\partial S}{\partial v} \parallel} \tag{12}$$

where $\wedge$ represent the product vector. The binormal vector b is calculated by:

$$b = n \wedge t \tag{13}$$

By integrating the tilt angle and the side tilt angle to the rotation matrix formed by the components of the Darboux mobile frame, the tool orientation angles (A, B, C) are calculated using the convention Z-Y-X Euler angles.

Once the poses extracted from the CAD path are determined, the inverse kinematics can be computed and the deflections along the path can be calculated using (6). The modified tool path to perform FSW consists on adding the

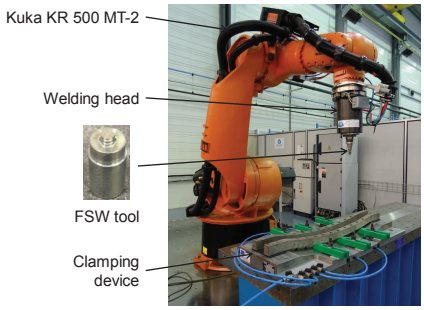

Fig. 4. RFSW experimental setup

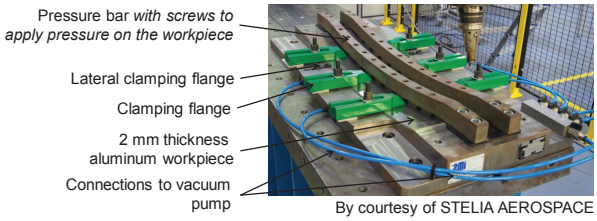

Fig. 5. Clamping device

deflections calculated to the poses extracted from the CAD path.

$$\boldsymbol{X}_{BP} = \boldsymbol{X}_{CAD} + \Delta\boldsymbol{X} \tag{14}$$

where $\boldsymbol{X}_{BP}$ is the modified path, $\boldsymbol{X}_{CAD}$ is the path extracted from the CAD model, $\Delta\boldsymbol{X}$ is determined by the deflection model. Finally, the modified tool path is approximated by n^{th} order Bézier curves and used to generate the robot program. Figure 3 summarizes the proposed path planning methodology.

4. EXPERIMENTAL VALIDATION

The experimental validation consists of performing a welding path with the proposed methodology on a test workpiece and analyzing the position and orientation accuracy obtained.

4.1 Experimental setup

The experiments were performed on a KUKA KR 500-2MT robot equipped with a welding head used for developing industrial applications at the Institut de Soudure, FSW center (Fig.4). The test workpiece, a 2 mm thick aluminum alloy EN AW-2024 T3, is placed inside the clamping device such that on all the length, the back of the plate perfectly fit on the clamping device (Fig. 5). The clamping device have also a vacuum field to ensure a proper fit-up between the workpiece and the anvil.
An FSW tool composed of a shoulder of 10 mm diameter and a pin of 1.9 mm is used for the experiments. The tilt angle is 2.5°. The robot is controlled in force in z tool direction (desired value $F_z = 8000\,\mathrm{N}$),the advance speed is $300\,mm/min$ and the rotation speed is $\Omega = 800$rpm. These welding parameters are assumed to be constant during the experiment and the thermal dissipation of the anvil is the same along the path. Therefore, the FSW wrench is supposed to be constant along the welding path. The forces induced in the lateral direction(F_y) and advance direction

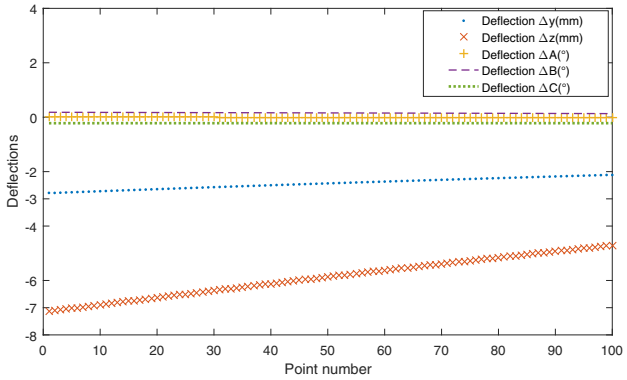

Fig. 6. Estimated deflections

(F_x) are 150 N and −420 N in the tool coordinate system, respectively. The torque in the axial direction (T_z) is 50 Nm.

4.2 Experiments, results and discussions

Considering the CAD model of the workpiece placed in the clamping device (Fig. 4) in which an arc of circular helix welding path is defined. This path is representative of an FSW path encountered in aeronautics. The position coordinates $(x_{CAD}, y_{CAD}, z_{CAD})$ of 100 points are extracted from the CAD model and then modeled by Bézier curves as described in the Section 3. Uniform parametrization method is chosen to calculate the Bézier parameter u. A 3^{th} order Bézier function does not permit to obtain an approximation precision under $\xi = 0.01$ mm and therefore, we compute 5^{th} order Bézier functions to approximate the position coordinates. The Bézier functions of the position coordinates are used to calculate orientation angles (A, B, C) with (11),(12),(13). Using the inverse kinematics and the deflection model (see (6)), we calculate the deflections along the welding path in the robot base coordinate system. We will not consider the deflection in the welding advance direction. Figure 6 shows the position deflections and the orientation deflections at each of the 100 points extracted from the CAD model. The deflection Δy represents the estimated tool lateral deviation along the the welding path. It will be added to y_{CAD} coordinate in order to compensate the lateral tool deviation. The deflection Δz, calculated in the axial direction, will be added to z_{CAD} coordinate in order to help the force controller to maintain easily the downforce at the desired value. The deflections $\Delta A, \Delta B, \Delta C$ represent the deviation of the tool orientation. For this application case, very small orientation deflections are calculated. Table 2 shows the RMS values of the calculated deflections.

By adding the deflections calculated to the poses extracted from the CAD model, we obtain a modified tool path which is also modeled by Bézier curves. We want to achieve an approximation precision $\xi = 0.01$ mm for the position coordinates and $\xi = 0.01°$ for the orientation angles. 5^{th} order Bézier curves permit to obtain the desired precision.

Table 2. RMS values of the deflections

Deflections	Δy	Δz	ΔA	ΔB	ΔC
RMS value	2.81 mm	5.95 mm	0.08°	0.16°	0.27°

Table 3. Coefficients of Bézier curves

Control points	P_0	P_1	P_2	P_3	P_4	P_5
P_x data [mm]	1521,13	1369,93	1218,72	1067,53	916,33	765,12
P_y data [mm]	2006,29	2002,40	1999,12	1995,28	1991,45	1987,51
P_z data [mm]	877,26	846,16	831,11	830,80	845,24	875,57
P_A data [°]	1.53	1.51	1.49	1.49	1.51	1.53
P_B data [°]	-9.08	-4.58	0.29	4.42	9.30	13.78
P_C data [°]	179,41	179,52	179,68	179,76	179,91	180,02

The control points calculated for each coordinate can be seen in Table 3. The CAD path and the modified tool path expressed in the robot base coordinate system can be seen in Figs. 7 and 8.

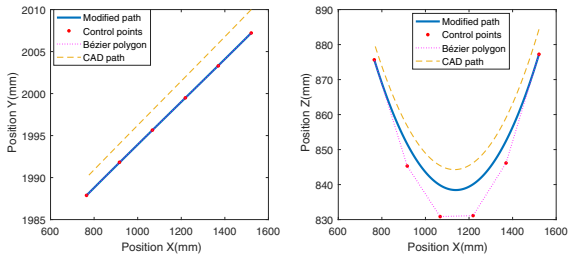

Fig. 7. Tool path in position

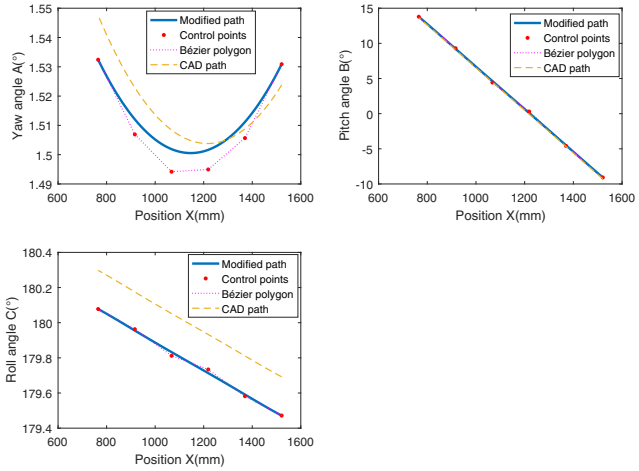

Fig. 8. Tool path for orientation angles

The modified tool path approximated by Bézier curves is then programmed in C++ on an external computer which is connected to the Kuka control system via an ethernet connection. A linear movement (LIN command) in the x direction is programmed in the Kuka control system from the beginning of the path(x_i) to the end(x_f). Each sampling time $T_s = 12\,ms$, the robot controller sends the x position to the external computer which calculates the parameter $u = \frac{x-x_i}{x_f-x_i}$ and then, sends to the robot the modified y, z positions and orientation angles A, B, C.

Figure 9 shows the weld seam obtained. In order to measure the lateral deviation with a microscope, a reference path corresponding to the desired X_{CAD} path was drawn in the weld seam with a tip tool. The lateral deviation is equal to the difference between the distance from the reference path to the border of the weld seam measured with a microscope and the radius of the tool shoulder (5 mm). The lateral deviations measured along the weld seam are under 0.5 mm (Fig. 10). The RMS value is 0.23 mm. To emphasize the result obtained, the same experiment is performed using RobotMaster, a classical offline programming software to generate the welding path without any deflections compensation. The RMS value of the lateral deviation obtained is 2.62 mm (Fig. 10). Therefore, our proposed methodology allows the improvement of the position accuracy about 91 %. The residual tool deviation measured along the seam is linked to the deflection model. It can tend towards null by taking into account more parameters such as the friction forces in the deflection model and a knowledge of the process forces with more precision. The orientation accuracy is determined by controlling the obtained weld seam. The visual (frontside and backside) and internal aspects of the weld seam do not reveal any defects. It implies that the orientation angles are correctly maintained during the welding.

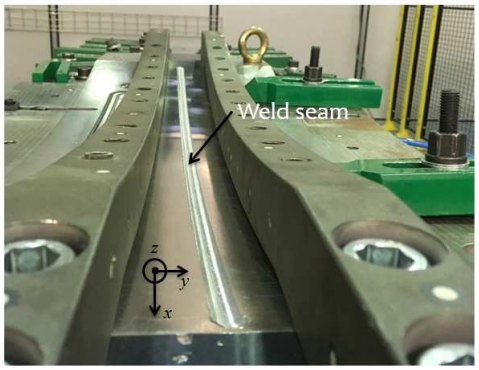

Fig. 9. Weld seam

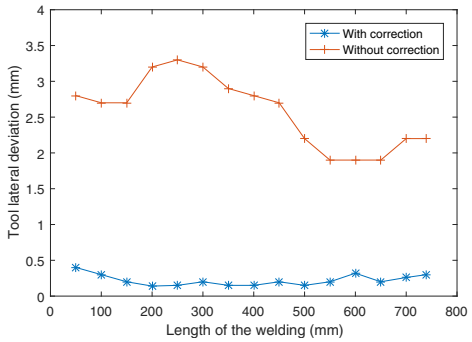

Fig. 10. Tool lateral deviation

5. CONCLUSIONS AND FUTURE WORK

In this paper, a feedforward compensation technique was presented for robotic friction stir welding. This technique is integrated in an offline path planning methodology which allows the generation of a welding tool position and orientation from CAD models and, at same time, the deflections

compensation of the robot subject to high process forces. The validation of the methodology on an arc of circular helix welding path allows the reduction of the lateral deviation from 2.62 mm to 0.23 mm. Good orientation of the welding tool was obtained, defect-free weld was performed. The pose accuracy can be improved with a knowledge of the process forces values with more precision and an improvement of the deflection model. Future work will be interested in experiencing the methodology to more complex 3D welding paths.

ACKNOWLEDGEMENTS

The authors would like to thank the O.N.E.R.A. for the financial support and Stelia Aerospace for providing the clamping device for the validation experiments.

REFERENCES

Bauer, J., Friedmann, M., Hemker, T., Pischan, M., Reinl, C., Abele, E., and von Stryk, O. (2013). Analysis of industrial robot structure and milling process interaction for path manipulation. In *Process Machine Interactions*, 245–263. Springer.

Belchior, J., Guillo, M., Courteille, E., Maurine, P., Leotoing, L., and Guines, D. (2013). Off-line compensation of the tool path deviations on robotic machining: Application to incremental sheet forming. *Robotics and Computer-Integrated Manufacturing*, 29(4), 58–69.

Besharati-Givi, M.K. and Asadi, P. (2014). *Advances in friction-stir welding and processing*. Elsevier.

Cook, G., Crawford, R., Clark, D., and Strauss, A. (2004). Robotic friction stir welding. *Industrial Robot*, 31(1), 55–63.

Cortsen, J. and Petersen, H.G. (2012). Advanced offline simulation framework with deformation compensation for high speed machining with robot manipulators. In *2012 IEEE/ASME International Conference on Advanced Intelligent Mechatronics (AIM)*, 934–939.

De Backer, J., Christiansson, A.K., Oqueka, J., and Bolmsj, G. (2012). Investigation of path compensation methods for robotic friction stir welding. *Industrial Robot*, 39(6), 601–608.

De Backer, J., Soron, M., IIal, T., and Christiansson, A. (2010). Friction stir welding with robot for light weight vehicle design. In *Proc. of 8th International Friction Stir Welding Symposium*, 14–24. Timmendorfer Strand, Germany.

Dumas, C., Caro, S., Garnier, S., and Furet, B. (2011). Joint stiffness identification of six-revolute industrial serial robots. *Robotics and Computer-Integrated Manufacturing*, 27(4), 881–888.

Giberti, H., Sbaglia, L., and Urgo, M. (2017). A path planning algorithm for industrial processes under velocity constraints with an application to additive manufacturing. *Journal of Manufacturing Systems*, 43, 160–167.

Jahanpour, J., Motallebi, M., and Porghoveh, M. (2016). A Novel Trajectory Planning Scheme for Parallel Machining Robots Enhanced with NURBS Curves. *Journal of Intelligent and Robotic Systems: Theory and Applications*, 82(2), 257–275.

Jubien, A., Abba, G., and Gautier, M. (2014). Joint stiffness identification of a heavy kuka robot with a low-cost clamped end-effector procedure. In *Proceedings of the 11th International Conference on Informatics in Control, Automation and Robotics, ICINCO 2014*, volume 2, 585–591. Vienna, Austria.

Khalil, W. and Dombre, E. (2004). *Modeling, Identification and Control of Robots*. Elsevier Ltd, Oxford.

Klimchik, A., Bondarenko, D., Pashkevich, A., Briot, S., and Furet, B. (2012). Compensation of tool deflection in robotic-based milling. In *ICINCO 2012 - Proceedings of the 9th International Conference on Informatics in Control, Automation and Robotics*, volume 2, 113–122.

Kusuda, Y. (2013). Honda develops robotized FSW technology to weld steel and aluminum and applied it to a mass-production vehicle. *Industrial Robot*, 40(3), 208–212.

Lyles, G., Honeycutt, J., and Cook, J. (2016). Status of NASA's Space Launch System. In *67th International Astronautical Congress*. Guadalajara, Mexico.

Mendes, N., Neto, P., Loureiro, A., and Moreira, A. (2016). Machines and control systems for friction stir welding: A review. *Materials and Design*, 90, 256–265.

Neubauer, M. and Müller, A. (2015). Smooth orientation path planning with quaternions using B-splines. In *IEEE/RSJ International Conference on Intelligent Robots and Systems (IROS)*, 2087–2092. IEEE.

Qin, J. (2013). *Robust Hybrid Position/Force Control of a Manipulator Used in Machining and in Friction Stir Welding (FSW)*. Phd thesis, in french, ENSAM, Metz, France.

Qin, J., Léonard, F., and Abba, G. (2014). Nonlinear discrete observer for flexibility compensation of industrial manipulators. In *The 19th IFAC World Congress*, volume 19, 5598–5604. Cap Town, South Africa.

Qin, J., Léonard, F., and Abba, G. (2016). Real-Time Trajectory Compensation in Robotic Friction Stir Welding Using State Estimators. *IEEE Transactions on Control Systems Technology*, 24(6), 2207–2214.

Shultz, E., Cole, E., Smith, C., Zinn, M., Ferrier, N., and Pfefferkorn, F. (2010). Effect of compliance and travel angle on friction stir welding with gaps. *Journal of Manufacturing Science and Engineering, Transactions of the ASME*, 132(4), 101–109.

Soron, M. and Kalaykov, I. (2006). A robot prototype for friction stir welding. In *2006 IEEE Conference on Robotics, Automation and Mechatronics*, 1–5. IEEE.

Tyapin, I., Kaldestad, K.B., and Hovland, G. (2015). Offline path correction of robotic face milling using static tool force and robot stiffness. In *2015 IEEE/RSJ International Conference on Intelligent Robots and Systems (IROS)*, 5506–5511.

Voellner, G., Zaeh, M., Silvanus, J., and Kellenberger, O. (2007). Robotic friction stir welding. *SAE Technical Papers*.

Zaeh, M. and Voellner, G. (2010). Three-dimensional friction stir welding using a high payload industrial robot. *Production Engineering*, 4(2), 127–133.

Zimmer-Chevret, S., Jemal, N., Langlois, L., Ben Attar, A., Hatsch, J., Abba, G., and Bigot, R. (2014). FSW process tolerance according to the position and orientation of the tool: Requirement for the means of production design. *Materials Science Forum*, 783-786, 1820–1825.